Physics of the Solid State, Vol. 47, No. 11, 2005, pp. 2196–2202. Translated from Fizika Tverdogo Tela, Vol. 47, No. 11, 2005, pp. 2106–2111.

FULLERENES AND ATOMIC CLUSTERS

Optimization of the Calculations of the Electronic Structure of Carbon Nanotubes

A. S. Fedorov and P. B. Sorokin

Kirensky Institute of Physics, Siberian Division, Russian Academy of Sciences, Akademgorodok, Krasnoyarsk, 660036 Russia

e-mail: alex99@akadem.ru

Received November 22, 2004

Abstract—A method is proposed for calculating the electronic structure and physical properties (in particular, Young's modulus) of nanotubes, including single-walled carbon nanotubes. This method explicitly accounts for the periodic boundary conditions for the geometric structure of nanotubes and makes it possible to decrease considerably (by a factor of $10–10^3$) the time needed to calculate the electronic structure with minimum error. In essence, the proposed method consists in changing the geometry of the structure by partitioning nanotubes into sectors with the introduction of the appropriate boundary conditions. As a result, it becomes possible to reduce substantially the size of the unit cell of the nanotube in two dimensions, so that the number of atoms in a new unit cell of the modified nanotube is smaller than the number of atoms in the initial unit cell by a factor equal to an integral number. A decrease in the unit cell size and the corresponding decrease in the number of atoms provide a means for drastically reducing the computational time, which, in turn, substantially decreases with an increase in the degree of partition, especially for nanotubes with large diameters. The results of the calculations performed for carbon and non-carbon (boron nitride) nanotubes demonstrate that the electronic structures, densities of states, and Young's moduli determined within the proposed approach differ insignificantly from those obtained by conventional computational methods. *© 2005 Pleiades Publishing, Inc.*

1. INTRODUCTION

The experimental discovery of carbon nanotubes in 1991 [1] has opened up new fields in applied and fundamental physics. Owing to their sizes (the transverse size is of the order of nanometers) and one-dimensional structure, carbon nanotubes exhibit unique mechanical, chemical, and electrical properties [2] and, already at present, have found wide applications in many areas of engineering. For example, since the invention of field-effect transistors based on carbon nanotubes in 1998, these devices have been fabricated in many laboratories and subjected to experimental tests [3, 4]. The unique combination of mechanical, elastic, and electrical (conductivity) properties of carbon nanotubes has allowed their use in tunneling and atomic-force microscopy. High hopes have been pinned on the design of ultrastrong fibers from carbon nanotubes (in particular, for practical implementation of the space elevator idea). Any technical application should be based on a detailed theoretical analysis. In this respect, theoretical investigations into the electrical and mechanical properties of nanotubes, the formation of defects in nanotube structures, and nanotube functionalization (i.e., the formation of chemical bonds between nanotubes and modifying molecules) are very important problems. Unfortunately, theoretical quantum-chemical investigations of nanotubes involve rather time-consuming procedures, primarily, because of the long time required for calculating the electronic structure of nanotubes with large diameters (which are most frequently encountered in experiments). For example, a unit cell of typical single-walled carbon nanotubes (SWCNTs), as a rule, contains from 10^1 to 10^2 atoms. However, in order to elucidate how defects of different types (adsorbed molecules, vacancies) affect the properties of single-walled carbon nanotubes, it is necessary to examine several unit cells; in this case, the minimum length of the region of the single-walled carbon nanotube under consideration is approximately equal to 10 Å. For this length, it is possible to avoid the undesirable effect exerted by defects in adjacent unit cells on each other; i.e., these defects are assumed to be isolated. Therefore, the study of any defects inside single-walled carbon nanotubes necessitates analysis of the structures in which the number of atoms ($\sim 10^2–10^3$) is one order of magnitude larger than that contained in the unit cell. The calculation of the electronic structure of these objects involves an extremely cumbersome procedure for any quantum-chemical (especially, *ab initio*) method, even for those that explicitly account for the periodic Bloch conditions, such as the methods based on the muffin-tin approximation (LMTO, FPLMTO, LAPW, etc.), the pseudopotential formalism, and other approaches. The computational time needed to calculate the electronic structure with these methods is proportional to $N^{\sim 2}–N^4$ (Hartree–Fock LCAO method), where N is the number of atoms in the unit cell in the structure under consideration. According to [5], one of

the fastest computational algorithms is provided by the pseudopotential method operating with the Vanderbilt ultrasoft pseudopotential [6], the plane-wave basis set, and the iterative diagonalization of the Hamiltonian in the framework of the density functional theory. In [5], it was demonstrated that, for systems containing up to 1000 electrons, the computational time of the algorithm is proportional to $\sim N^2$. However, we can assume that, even in the calculations performed with the above method for nanotubes having large diameters, the considerable decrease in the size of the computational cell and in the number of atoms in it is of crucial importance in the case when this does not lead to substantial errors due to the transformation of the cell.

2. COMPUTATIONAL TECHNIQUE

In this paper, we propose a technique that makes it possible to reduce considerably the time needed to calculate the electronic structure of nanotubes. This approximation is based on a change in the nanotube geometry and allows one to decrease substantially the size of the unit cell of the nanotube and the number of atoms in the cell. By assuming that the method is used to perform calculations in a plane-wave basis set in which the wave function is calculated in different spatial regions, including those with an almost zero value, the proposed algorithm enables one to avoid calculations of the electron density in the vicinity of the nanotube axis where the electron density is virtually zero ($\rho \approx 0$) and, thus, to additionally increase the computational speed. The applicability of the method is illustrated by calculating a number of single-walled carbon nanotubes and a (10, 10) single-walled boron nitride nanotube.

The key idea underlying this method is that the electronic structures of a single-walled carbon nanotube and a graphite sheet are similar to each other. Only for single-walled carbon nanotubes with very small diameters ($D \le 6$ Å) are the electronic structures of graphite and single-walled carbon nanotubes somewhat different. A comparison of the geometric structures of the graphite sheet and the single-walled carbon nanotube shows that the fundamental difference between them lies in the boundary conditions. The graphite sheet is treated as an infinite plane, and the boundary conditions for the electron wave functions are specified using the Bloch theorem. The electron wave function depends on the two-dimensional wave vector $k = \{k_x, k_y\}$ aligned parallel to the graphite sheet. For a single-walled carbon nanotube, the boundary conditions are similar to those for graphite only along the nanotube axis (the Z axis).

Let us consider the wave vector k_x along the rolled graphite sheet perpendicular to the nanotube axis. It is evident that, in this case, the wave vector changes discretely as a result of the periodicity when tracing around the circumference of the nanotube.

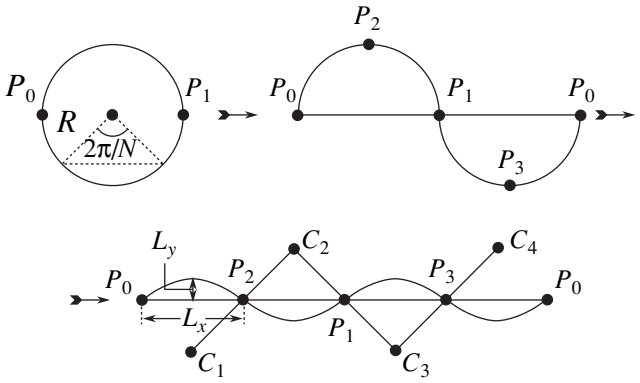

Fig. 1. Sequential transformation of a nanotube sector into a corrugated surface.

The symmetry group of the (n, n) and (n, 0) nanotubes contains the rotation axes [7, 8]:

$$\begin{cases} D_{nh} : N = 2m \\ D_{nd} : n = 2m + 1, \quad m = 1, 2\ldots. \end{cases}$$

Hence, the nanotube can be separated into n equivalent sectors [9].

Chiral nanotubes of the (n, m) type are characterized by the symmetry group $G = \mathbf{C}_d \otimes \mathbf{C}'_{Nd/\Omega}$, where $\mathbf{C}_d = \{C_d, C_d^2, \ldots, C_d^2 = E\}$ and d is determined by the following conditions:

$$\begin{cases} mp - nq = d \\ q < m/d \\ p < n/d. \end{cases}$$

Owing to the screw axes, the chiral nanotube can be separated into d equivalent sectors with the corresponding increase in their period along the Z axis.

The periodicity of the nanotube geometry enables us to change the geometry of the calculated structure by separating the structure of the nanotube into equivalent sectors and reflecting each subsequent sector with respect to the plane tangential to the adjacent sectors along the line of their contact. Figure 1 illustrates this sequential transformation of the single-walled carbon nanotube into corrugated surfaces consisting of two and then four sectors with the exact same curvature as that of the initial geometric structure of the single-walled carbon nanotube. The projections of the nanotube and two corrugated surfaces onto the plane perpendicular to the nanotube axis are also depicted in Fig. 1. The $C_i - C_{i+1}$ lines are perpendicular to the reflection planes of the sectors whose reflection provides the formation of the corrugated surface. The points P_i are the projections of the contact lines of sequential sectors. At the first stage of the nanotube transformation, the initial single-

walled carbon nanotube is transformed into the simplest corrugated surface by reflecting the half-sector of the nanotube with respect to the plane passing through the line of contact (with the projection P_1). Then, this structure is transformed into the next corrugated surface by reflecting the previous corrugated surface with respect to two planes (passing through the lines with the projections P_2 and P_3). The partition of the corrugated surfaces can be repeated. In this case, if the number of reflection planes is equal to M, the number N of equivalent sectors of the corresponding corrugated surface formed from the nanotube structure is $N = M + 1$.

Since the single-walled carbon nanotube is partitioned into a number of periodically repeated sectors located along the X axis, it is possible to calculate the electronic structure only for one sector of the corrugated surface. An increase in the degree of partition of the nanotube leads to a decrease in the unit cell of the corrugated surface. This results in an increase in the computational speed. Proper allowance must be made for the fact that the periodicity of the corrugated surface along the X axis leads to a dependence of the electron wave function $\psi^{\nu}(r)$ (where $\nu = \{k_x, k_z, n\}$ and n is the number of the band) on the wave vector component k_x. The wave vector k of the nanotube has only one component (along the nanotube axis), whereas the wave vector k of the corrugated surface has two components (k_x, k_z). Note that the inclusion of the boundary conditions (periodicity) for the wave function when tracing around the circumference of the nanotube leads to the sole possible set $k_{xi} = \{2\pi i/L_x N, i = 0\ldots(N-1)\}$(where L_x is the period of the corrugated surface along the x direction).

The structure of the corrugated surface differs from the structure of the single-walled carbon nanotube only in that the curvature of the corrugated surface changes jumpwise (only in sign) along a small number of lines with the projections P_i. Therefore, it can be expected that any wave eigenfunction $\psi^{\nu}(r)$ ($\nu = \{k_x, k_z, n\}$ of an electron traveling along the corrugated surface should be similar to a wave function of an electron traveling along the surface corresponding to the single-walled carbon nanotube.

It should be noted that the number of atoms in the unit cell of the corrugated surface is smaller than the number of atoms in the unit cell of the single-walled carbon nanotube by a factor of N. In this case, an increase in the set of possible values of the quasimomentum k_x by a factor of N restores the total number of possible electron eigenstates in the nanotube.

It is interesting to estimate the gain in the computational speed that can be achieved with the use of the proposed approximation as compared to the conventional calculation of nanotubes. We assume that, in the case of single-walled carbon nanotubes with large radii R, the chosen unit cell size determined by the periods L_x and L_y is considerably larger than the vacuum gap between the adjacent nanotubes. Under this assumption with due regard for the schematic diagram depicted in Fig. 1, it is easy to derive the relationships $L_x = 2R\sin(\pi/N)$ and $L_y = R(1 - \cos(\pi/N))$. Taking into account that, in the proposed method, the computational speed V is proportional to $O(N_{\text{at}}^{-2})$ (where N_{at} is the number of atoms in the unit cell) and the number of atoms in the unit cell depends linearly on the unit cell volume, we obtain the formula

$$\frac{V_{\text{tube}}}{V_{CSS}} \sim \left(\frac{\Omega_{\text{tube}}}{\Omega_{CSS}}\right)^2 = \left(\frac{(2R)^2 L_z}{L_x L_y L_z}\right)^2$$
$$= \left(\frac{2}{\sin(\pi/N)(1-\cos(\pi/N))}\right)^2.$$

For $N \gg \pi$, the computational speed is proportional to $V_{\text{tube}}/V_{CSS} \sim 2N/\pi$. The increase in the number of wave vector components k_x in the corrugated surface is compensated for by the decrease in the number of atoms in its unit cell.

3. THE ORIGIN OF POSSIBLE ERRORS OF THE METHOD

It is very important to reveal the origin of possible errors in the calculation of the electronic structure after the transformation of the carbon nanotube into a corrugated surface. It is clear that possible errors are associated with the change in the curvature of the structure under consideration. It is this curvature of the rolled graphite sheet that is responsible for the small differences between the electronic structures of the nanotube and the graphite sheet. The analysis of the corrugated surface in the cylindrical coordinates relative to the rotation axes (see the projections of the C_i axes in Fig. 1) demonstrates that the first derivative of the coordinates of the point on the corrugated surface with respect to the rotation angle is continuous and that the curvature determined by the second derivative of the coordinates vanishes along the lines whose projections in Fig. 1 are represented by the points P_i. At other points of the corrugated surface, the curvature coincides in magnitude with the curvature of the single-walled carbon nanotube. To put it differently, the transformation of the geometric structure of the nanotube into the corrugated surface in terms of the solutions to the Schrödinger equation is a correct procedure at all points except for the points of the contact lines of the sectors (with the projections P_i), which simultaneously belong to two different sectors of the corrugated surface and in which the curvature vanishes.

The origin of the errors can be revealed directly from analyzing the differential Schrödinger equation

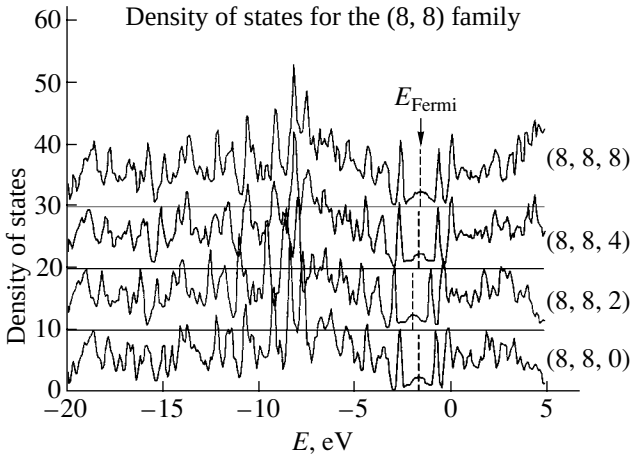

Fig. 2. Densities of states for the (8, 8, *i*) structures at *i* = {0, 2, 4, 8}.

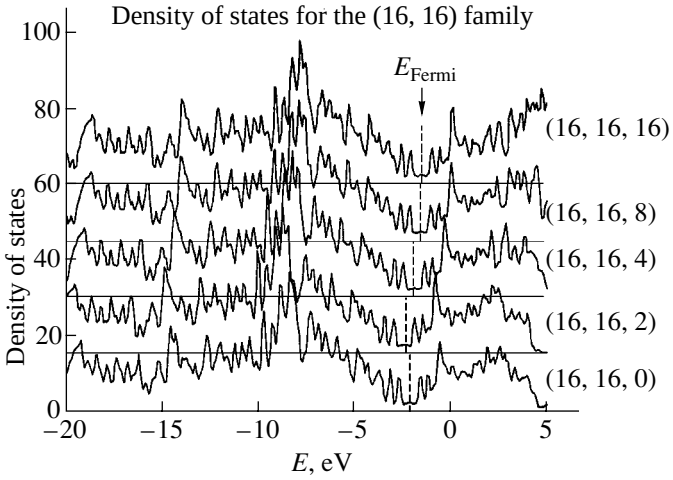

Fig. 3. Densities of states for the (16, 16, *i*) structures at *i* = {0, 2, 4, 8, 16}.

by writing the Laplacian in the cylindrical coordinates:

$$-\left[\frac{\nabla^2}{2m} + \hat{V}(r)\right]\Psi^{\nu}(r) = \varepsilon^{\nu}\Psi^{\nu}(r), \quad \nu = \{k, n\},$$
$$\nabla^2 = \frac{\partial^2}{\partial\rho^2} + \frac{1}{\rho}\frac{\partial}{\partial\rho} + \frac{1}{\rho^2}\frac{\partial}{\phi^2} + \frac{\partial^2}{\partial z^2}. \quad (1)$$

Now, we take into account that $C_3P_1 = -C_2P_1$ and that the first and second derivatives in the Laplacian have the difference approximations $\partial y_i/\partial\rho \simeq 1/2h(-y_{i-1} + y_{i+1})$ and $\partial^2 y_i/\partial\rho^2 \simeq (1/h^2)(16y_{i-1} - 2y_i + y_{i+1})$. Then, it becomes clear that all the terms in the Laplacian are continuous functions of the arguments (ρ, ϕ), except for the term $(1/\rho)\partial/\partial\rho$ that changes the sign along the contact lines P_i. This term is the sole factor responsible for the possible change in the Laplacian upon transformation of the single-walled carbon nanotube into the corrugated surface. Fortunately, it follows from relationship (1) that this term decreases in proportion to the increase in the nanotube radius. Consequently, when the diameter of the initial nanotube is sufficiently large and the number of points P_i is small, we can expect that the electronic structure of the corrugated surface will virtually coincide with the electronic structure of the single-walled carbon nanotube.

4. CALCULATIONS OF THE ELECTRONIC STRUCTURE OF CORRUGATED SURFACES

As an example, we calculated the electronic structures of single-walled carbon nanotubes with different diameters and chiralities and also the electronic structures of the corresponding corrugated surfaces. The band structures, densities of states, and binding energies were calculated for the (20, 0) zigzag single-walled carbon nanotube (according to the notations proposed in [10]) and the (8, 8) and (16, 16) armchair single-walled carbon nanotubes.

All the calculations were performed with the Vienna Ab Initio Simulation Package (VASP) [5, 11, 12]. This program package makes it possible to perform *ab initio* calculations based on the pseudopotential method and a plane-wave basis set in the framework of the local density functional formalism [13, 14]. The use of the Vanderbilt pseudopotentials in the calculations led to a substantial decrease (to 287 eV) in the maximum kinetic energy E_{cutoff} of the plane-wave basis set without a significant loss of accuracy. The electron–electron exchange and correlation interactions were described by the functional density theory method with the Ceperley–Alder exchange–correlation functional [15], which has worked well in similar calculations.

All the geometric structures of the nanotubes and the corresponding corrugated surfaces were constructed on the basis of the graphite sheet (with an interatomic distance of 1.42 Å) curved in a specific manner. The densities of states for all the structures under investigation are shown in Figs. 2–4. In these figures, the corrugated surfaces are designated by the indices (*i*, *j*, *k*), where *k* is the number of sectors into which the nanotube is partitioned upon transformation into a corrugated surface and (*i*, *j*) are the chirality indices. For example, the designation (8, 8, 0) corresponds to the initial (8, 8) single-walled carbon nanotube and the designation (8, 8, 4) refers to the corrugated surface obtained by partitioning the initial nanotube into four sectors. It can be seen from Figs. 2–4 that the densities of states for all the corrugated surfaces almost coincide with the density of states for the initial nanotube. This indicates an insignificant contribution from a finite number of lines in which the curvature of the geometric structures of the single-walled carbon nanotube and the corrugated surfaces differ from each other.

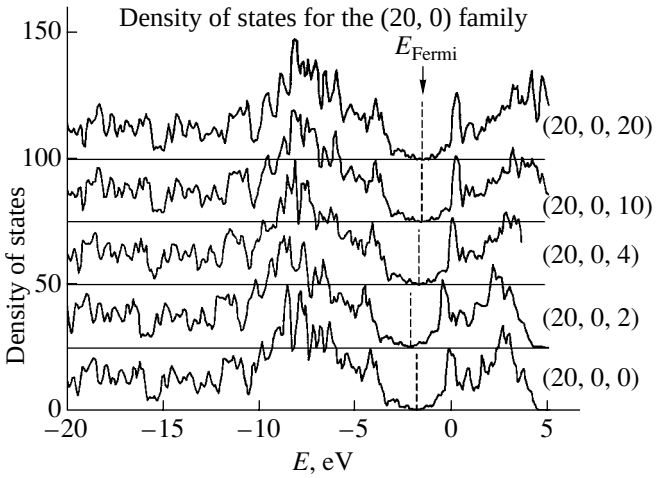

Fig. 4. Densities of states for the (20, 0, *i*) structures at *i* = {0, 2, 4, 10, 20}.

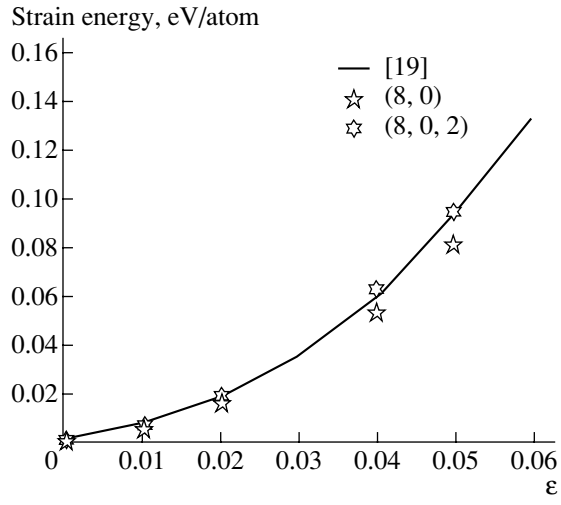

Fig. 5. Dependences of the strain energy on the strain for the (8, 0) single-walled carbon nanotube and the (8, 0, 2) corrugated surface.

Moreover, we investigated how the optimization of the geometry structure affects the electronic structures of all the objects. For this purpose, the electronic characteristics were calculated for the structures with optimized and unoptimized geometries. All the degrees of freedom of atomic coordinates could be varied in the course of optimization. The optimization was carried out by the conjugate-gradient method. The structure was treated as optimized when the magnitude of the force acting on any atom was less than 0.02 eV/Å. The calculations demonstrated that the densities of states for the optimized structures are in close agreement with the densities of states for the corresponding unoptimized structures. For this reason, these densities of states are not presented in the figures.

The total binding energies (per atom) for all the structures (optimized and unoptimized) are listed in Table 1. The computational times of one iteration (over all *k* points), the numbers of *k* points, and the numbers of plane waves (averaged over the *k* points) are also presented in Table 1. The calculations were carried out on a PIII-860 personal computer. As can be seen from Table 1, the binding energies for the corrugated surfaces are very close to the binding energies for the corresponding single-walled carbon nanotubes. Note that the difference between these energies increases with an increase in the degree of partition of the nanotubes. It can also be seen from these data that, in all cases, the binding energy depends very weakly on the optimization of the structure.

5. APPLICATION OF THE CORRUGATED-SURFACE METHOD FOR CALCULATING THE ELASTIC PROPERTIES OF NANOTUBES

The proposed method was also used to calculate the elastic properties of carbon and non-carbon structures. The Young's moduli Y were calculated for the (6, 6) and (10, 10) single-walled carbon nanotubes. The Young's moduli of the nanotubes, as a rule, have been calculated from the standard formula $Y = (1/V_0)(\partial^2 E/\partial\varepsilon^2)$, where $V_0 = 2\pi LR\delta R$ is the volume of the unstrained structure and δR is the thickness of the nanotube wall. However, there is arbitrariness in choosing the thickness of the nanotube wall δR. For example, Lu [16] determined the thickness of the nanotube wall δR as the distance between the graphite sheets, whereas Yakobson *et al.* [17], reasoning from the atomic radius of carbon, assumed that the thickness δR is equal to 0.66 Å. This problem was solved by Hernandez *et al.* [18], who introduced the modified Young's modulus $Y_s = (1/S_0)(\partial^2 E/\partial\varepsilon^2)$, where $S_0 = 2\pi LR$. It is this relationship that was used in the present work.

The calculated Young's moduli Y_s are given in Table 2. It can be seen from this table that, in the case of the (6, 6) single-walled carbon nanotube with a small diameter, the error in the calculation of the Young's moduli Y_s for the corrugated structure is rather large. However, as the nanotube diameter increases, the accuracy of the calculation increases in accordance with the predictions made in Section 2. In addition to the calculations of the elastic properties of the armchair carbon nanotubes, we calculated the strain energy (i.e., the energy associated with the bending of the graphite sheet upon formation of the nanotube) for the (8, 0) zigzag single-walled carbon nanotube and the corresponding (8, 0, 2) corrugated surface. The results obtained are presented in Fig. 5 (the dependence shown by the solid line is taken from [19]).

It can be seen from Fig. 5 that the strain energies of the initial single-walled carbon nanotube and the corresponding corrugated surface are very close to each other (at moderate strains). This indicates that the pro-

Table 1. Binding energies per atom (eV) for the (8, 8, *i*), (16, 16, *i*), and (20, 0, *i*) structures; numbers of *k* points; numbers of plane waves; and times of one iteration for the calculation of the (20, 0, *i*) structures

(8, 8, *i*) *i* = 0, 2, 4, 8	9.340	9.356	9.375	9.390	–
(optimized/unoptimized)	9.331	9.340	9.347	9.364	–
(16, 16, *i*) *i* = 0, 2, 4, 8, 16	9.390	9.392	9.393	9.406	9.405
(optimized/unoptimized)	9.381	9.348	9.381	9.385	9.389
(20, 0, *i*) *i* = 0, 2, 4, 10, 20	9.304	9.308	9.318	9.336	9.336
(optimized/unoptimized)	9.304	9.307	9.310	9.321	9.331
Number of *k* points	14	28	42	84	154
Number of plane waves	26290	15216	6290	2350	1158
Time of one iteration (s)	88517	40037	12340	2500	890

Table 2. Young's moduli Y_S (TPa nm) calculated for the carbon and non-carbon structures

SWCNT	Y_S	SWCNT	Y_S	SWCNT	Y_S	BN nanotube	Y_S
(6, 6)	0.463	(8, 0)	0.437	(10, 10)	0.423	(10, 10)	0.316
(6, 6, 2)	0.546	(8, 0, 2)	0.455	(10, 10, 2)	0.439	(10, 10, 2)	0.329
[14]	0.415	[14]	–	[14]	0.423	[14]	0.306

posed method can be used for calculating not only the electronic structure but also the elastic properties of carbon nanotubes.

Apart from the calculations of the properties of the single-walled carbon nanotubes, we calculated some properties for a number of boron nitride (BN) nanotubes. In particular, we calculated the binding energies for the (10, 10) nanotube and the (10, 10, 2) corrugated surface, as well as the Young's moduli for these structures (Table 2). The results obtained demonstrate that, within the proposed approach, the properties of non-carbon structures are described with a high accuracy.

6. CONCLUSIONS

Thus, we proposed a method for calculating the electronic structure and elastic properties of nanotubes, including single-walled carbon nanotubes. This method makes it possible to accelerate the calculations significantly. The proposed approach is based on modification of the geometry of the calculated nanotube through a local piecewise change in its curvature and on the introduction of additional boundary conditions. This provides a means for calculating the corrugated surface with a unit cell having considerably smaller transverse sizes. Moreover, the number of atoms in the unit cell of the new corrugated surface is *N* times smaller than that in the nanotube. The applicability of the method was illustrated by calculating the electronic structure for a number of carbon and non-carbon (boron nitride) single-walled nanotubes. It was shown that the time it takes for the nanotube properties to be calculated decreases considerably (by a factor of $10–10^3$ depending on the diameter) as the degree of partition of the single-walled carbon nanotube increases, especially for nanotubes with large diameters. A detailed analysis of the Hamiltonian along the lines of the piecewise change in the nanotube curvature demonstrated that the proposed approach leads to an insignificant difference between the calculated structures of the nanotube and the corresponding corrugated structure. This difference decreases in proportion to the increase in the radius of the carbon nanotube.

ACKNOWLEDGMENTS

We would like to thank the Institute of Computer Modeling (Siberian Division, Russian Academy of Sciences, Russia) for providing the opportunity to use a cluster computer for performing the quantum-chemical calculations.

This work was supported in part by the Russian federal program "Integration," project nos. B0017 and Ya0007.

REFERENCES

1. S. Ijima, Nature (London) **354**, 56 (1991).
2. P. M. Ajayan and T. W. Ebbesen, Rep. Prog. Phys. **60**, 1025 (1997).
3. S. J. Tans, A. R. M. Verschueren, and C. Dekeer, Nature (London) **393**, 49 (1998).
4. Ph. Avouris, R. Martel, S. Heinze, M. Radosavljevec, S. Wind, V. Derycke, J. Appenzeller, and J. Terso, in *Proceedings of the XVI International Winter School on Electronic Properties of Novel Materials, Kirchberg Winter School, Tyrol, Austria, 2002*, Ed. by H. Kuzmany, J. Fink, M. Mehring, and S. Roth (AIP, Melville, NY, 2002).

5. G. Kresse and J. Furthmüller, Phys. Rev. B: Condens. Matter **54** (16), 11169 (1996).
6. D. Vanderbilt, Phys. Rev. B: Condens. Matter **41** (11), 7892 (1990).
7. R. A. Jishi, L. Venkataraman, M. S. Dresselhaus, and G. Dresselhaus, Chem. Phys. Lett. **209**, 77 (1993).
8. R. A. Jishi, M. S. Dresselhaus, and G. Dresselhaus, Phys. Rev. B: Condens. Matter **47** (24), 16671 (1993).
9. G. Ya. Lyubarskii, *The Application of Group Theory in Physics* (GITTL, Moscow, 1957; Pergamon, New York, 1960).
10. C. T. White, D. H. Robertson, and J. W. Mintmire, Phys. Rev. B: Condens. Matter **47** (9), 5485 (1993).
11. G. Kresse and J. Hafner, Phys. Rev. B: Condens. Matter **47** (1), 558 (1993).
12. G. Kresse and J. Hafner, Phys. Rev. B: Condens. Matter **49** (20), 14251 (1994).
13. P. Hohenberg and W. Kohn, Phys. Rev. **136** (3B), B864 (1964).
14. W. Kohn and L. J. Sham, Phys. Rev. **140** (4A), A1133 (1965).
15. D. M. Ceperley and B. J. Alder, Phys. Rev. Lett. **45** (14), 566 (1980).
16. J. P. Lu, Phys. Rev. Lett. **79** (7), 1297 (1997).
17. B. I. Yakobson, C. J. Brabec, and J. Bernholc, Phys. Rev. Lett. **76** (14), 2511 (1996).
18. E. Hernandez, C. Goze, and P. Bernier, Appl. Phys. A: Mater. Sci. Process. **68** (24), 287 (1999).
19. D. Srivastava, M. Menon, and K. Cho, Phys. Rev. Lett. **83** (15), 2973 (1999).

Translated by O. Borovik-Romanova